Structural, Vibrational, and Electronic Characteristics of Enyne Macrocycles as a Function of Ring Strain

Sara Eisler, Robert McDonald, Glen R. Loppnow, and Rik R. Tykwinski*

Contribution from the Department of Chemistry, University of Alberta, Edmonton, Alberta, T6G 2G2 Canada

Received February 21, 2000

Abstract: The cross-conjugated macrocycles **8a**−**e** and acyclic model compound **12** have been synthesized and thoroughly analyzed by ^{1}H and ^{13}C NMR, UV, IR, and Raman spectroscopies, and by X-ray crystallography. The increasing ring strain and resultant changes in the double and triple bond orders are clearly detailed in the Raman and ^{13}C NMR spectra, as well as in the X-ray structures. Correlations between ^{13}C NMR shifts, bond angles, and Raman frequencies are essentially linear for the butadiynyl and olefinic moieties. The most highly strained system, **8a**, displays interior alkylidene bond angles that are reduced to 108° and alkyne angles reduced to as little as 155°. The electronic absorption spectrum of **8a** shows evidence of through-space homoconjugation that is manifested as a bathochromic shift of the absorption band arising from the in-plane π-system. The absorption bands from the out-of-plane π-electron systems of the more strained cycles **8a** and **8b** show slight bathochromic shifts as compared with the less strained systems **8c**−**e** and acyclic **12**. Ring strain, however, has a surprisingly small effect on the electronic absorption energies of these macrocycles.

Introduction

The sp-hybridization of carbon in an alkyne moiety dictates a linear geometry for the C−C≡C bond. The fact that this angle is considerably more flexible than either a C−C=C or C−C−C bond allows for fairly large deviations from 180° to occur without significant changes in energy.[1] As a result, Krebs has gone so far as to specify that only compounds in which the C−C≡C bond angle has been reduced to less than 170° are even considered strained.[1] The first strained cycloalkynes, cyclononyne[2] and cyclooctyne,[3] reported in the early 1950s by Blomquist, ushered in an era of fascination with the synthesis and study of cyclic alkynes and enynes. Almost five decades later, the aesthetically pleasing structures and interesting chemical and biological[4] reactivity of these macrocycles continue more than ever to capture the imagination of chemists.[1,5−17]

Cyclic enynes are a particularly interesting category of strained alkynes.[18] Included in this category are dehydroannulenes and dehydrobenzoannulenes (DBAs), molecules that have been widely studied since Sondheimer's seminal work almost 30 years ago.[12,14,19] Within the large range of known DBAs are examples of the most strained alkynes to be characterized, some with bond angles of less than 155°, i.e., **1**.[20] Recently, the ring strain in DBAs such as **2** has been harnessed for the formation of polydiacetylene polymers and carbon nanostructures via thermal topochemical polymerization.[21−24]

Enyne macrocycles and related cage compounds play a key role in current synthetic endeavors toward C_{60} and other fullerenes.[17,25−30] Typically, these approaches utilize suitably functionalized precursors to afford cyclic polyynes that could enter into a polyyne cyclization mechanism, ultimately expected to yield a fullerene product. It is assumed that this reaction

* To whom correspondence should be addressed. E-mail: rik.tykwinski@ualberta.ca.

(1) Krebs, A.; Wilke, J. *Top. Curr. Chem.* **1983**, *109*, 189−233.
(2) Blomquist, A. T.; Liu, L. H.; Bohrer, J. C. *J. Am. Chem. Soc.* **1952**, *74*, 3643−3647.
(3) Blomquist, A. T.; Liu, L. H. *J. Am. Chem. Soc.* **1953**, *75*, 2153−2154.
(4) Nicolaou, K. C.; Smith, A. L. In *Modern Acetylene Chemistry*; Stang, P. J., Diederich, F., Eds.; VCH: Weinheim, 1995; pp 203−283.
(5) *Modern Acetylene Chemistry*; Stang, P. J., Deiderich, F., Eds.; VCH: Weinheim, 1995.
(6) Carbon Rich Compounds II. *Top. Curr. Chem.* **1999**, *201* (special issue).
(7) Moore, J. S. *Acc. Chem. Res.* **1997**, *30*, 402−413.
(8) (a) Tykwinski, R. R.; Diederich, F. *Liebigs Ann./Recl.* **1997**, 649−661. (b) Diederich, F. *Nature (London)* **1994**, *369*, 199−207. (c) Diederich, F.; Rubin, Y. *Angew. Chem., Int. Ed. Engl.* **1992**, *31*, 1101−1123.
(9) Sander, W. *Angew. Chem., Int. Ed. Engl.* **1994**, *33*, 1455−1456.
(10) (a) Gleiter, R.; Schäfer, W. In *The Chemistry of Triple-Bonded Functional Groups: Supplement C2*; Patai, S., Ed.; John Wiley & Sons: Chichester, 1994; Vol. 2, pp 153−189. (b) Gleiter, R. *Angew. Chem., Int. Ed. Engl.* **1992**, *31*, 27−44.
(11) Nakagawa, M. In *The Chemistry of the Carbon−Carbon Triple Bond*; Patai, S., Ed.; John Wiley & Sons: Chichester, 1978; pp 635−712.
(12) Haley, M. M. *Synlett* **1998**, 557−565.
(13) Scott, L. T. *Pure Appl. Chem.* **1986**, *58*, 105−110.
(14) Hoffmann, R. W. *Dehydrobenzene and Cycloalkynes*; Academic Press: New York, 1967.
(15) Sakurai, H.; Nakadaira, Y.; Hosomi, A.; Eriyama, Y.; Kabuto, C. *J. Am. Chem. Soc.* **1983**, *105*, 3359−3360.
(16) Rubin, Y. *Chem. Eur. J.* **1997**, *3*, 1009−1016.
(17) Bunz, U. H. F.; Rubin, Y.; Tobe, Y. *Chem. Soc. Rev.* **1999**, 107−119.
(18) (a) Meier, H.; Hanold, N.; Molz, T.; Bissinger, H. J.; Kolshorn, H.; Zountsas, J. *Tetrahedron* **1986**, *42*, 1711−1719. (b) Meier, H.; Petersen, H.; Kolshorn, H. *Chem. Ber.* **1980**, *113*, 2398−2409.
(19) Sondheimer, F. *Acc. Chem. Res.* **1972**, *5*, 81−91.
(20) de Graaff, R. A. G.; Gorter, S.; Romers, C.; Wong, H. N. C.; Sondheimer, F. *J. Chem. Soc., Perkin Trans. 2* **1981**, 478−480.
(21) Baldwin, K. P.; Matzger, A. J.; Scheiman, D. A.; Tessier, C. A.; Vollhardt, K. P. C.; Youngs, W. J. *Synlett* **1995**, 1215−1218.
(22) Zhou, Q.; Carroll, P. J.; Swager, T. M. *J. Org. Chem.* **1994**, *59*, 1294−1301.
(23) Boese, R.; Matzger, A. J.; Vollhardt, K. P. C. *J. Am. Chem. Soc.* **1997**, *119*, 2052−2053.
(24) Dosa, P. I.; Erben, C.; Iyer, V. S.; Vollhardt, K. P. C.; Wasser, I. M. *J. Am. Chem. Soc.* **1999**, *121*, 10430−10431.
(25) Kiang, C.-H.; Goddard,W. A., III. *Phys. Rev. Lett.* **1996**, *76*, 2515−2518.
(26) Rubin, Y.; Parker, T. C.; Pastor, S. J.; Jalisatgi, S.; Boulle, C.; Wilkins, C. L. *Angew. Chem., Int. Ed.* **1998**, *37*, 1226−1229.

10.1021/ja000617g CCC: $19.00
Published on Web 07/11/2000

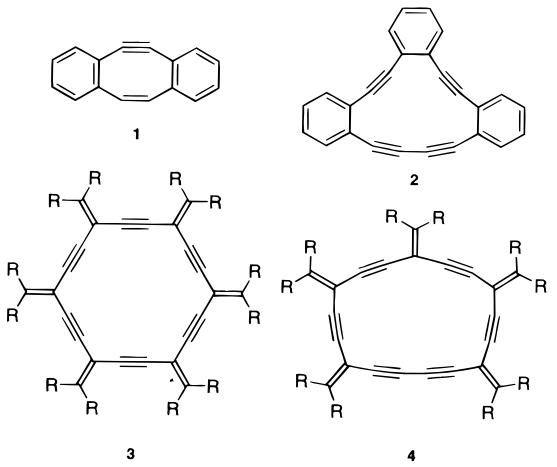

sequence is initiated as a result of the reactivity and ring strain of the polyyne intermediate.[8b,c,31]

In the above examples and in the majority of reports concerning strained cyclic acetylenes, it has been the stability and/or reactivity as a function of ring strain that has been examined. Comparatively, the electronic aspects of strained alkynes have been much less studied.[32,33] For nonconjugated systems, extensive studies by Gleiter and co-workers have determined the electronic effects of ring strain for isolated ethynes and butadiynes.[10,34] Scott, de Meijere, and co-workers have reported on the electronic effects of homoconjugation in a range of macrocyclic polyacetylenes.[6,13,35] Neither these studies, nor others,[11,36,37] however, have provided significant insight into the structural and electronic attributes of cyclic alkynes with extended conjugation. As the role of alkynes in assembling highly conjugated systems for materials applications has increased dramatically during the past decade,[5,6] an understanding of electronic and structural characteristics based on angular distortions is essential.

Scheme 1. Synthesis of Macrocycles **8a**−**e**

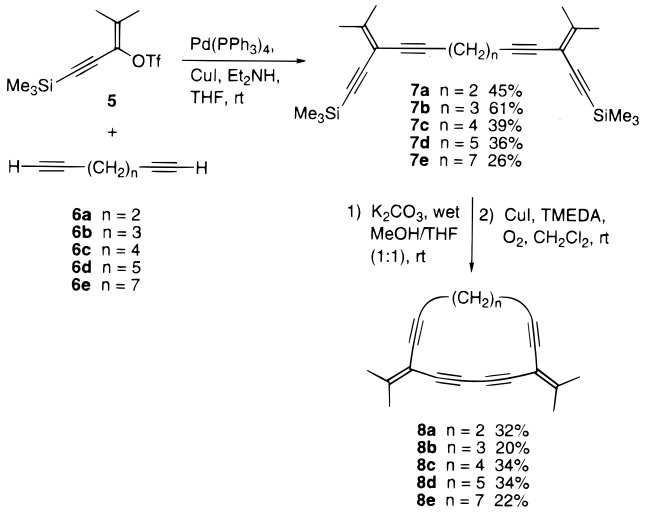

In the course of investigating the effects of cross conjugation in expanded radialenes such as **3** and **4**,[38] it became necessary to assess the influence of ring strain on these and related molecules.[39] Since the degree of conjugation could be enhanced, diminished, or otherwise altered in strained structures, our ability to assess electronic changes as a function of molecular structure was viewed as fundamental toward tuning and tailoring the bulk properties of these new organic materials. In particular, the effects of strain for conjugated macrocycles containing a butadiyne segment,[21−24] such as in **4**, held specific appeal due to the rich history of this moiety in the formation of polydiacetylenes.[40−42] Reported herein are the syntheses and characterization of a surprisingly stable series of cross-conjugated, enyne macrocycles, **8a**−**e**,[38,43] also deemed cyclic expanded dendralenes,[44] and the acyclic model compound **12**. The extent and effects of ring strain in these macrocycles have been thoroughly examined by ^{13}C NMR, Raman, and UV−vis spectroscopies, as well as X-ray crystallography for all six molecules **8a**−**e** and **12**.

Results and Discussion

Syntheses. The cyclic expanded dendralenes **8a**−**e** were constructed as outlined in Scheme 1. Diynes **6a**−**e** were coupled with vinyl triflate **5**[45] (2.2 equiv) in the presence of Et_2NH, CuI,

(27) Tobe, Y.; Fujii, T.; Matsumoto, H.; Tsumuraya, K.; Noguchi, D.; Nakagawa, N.; Sonoda, M.; Naemura, K.; Achiba, Y.; Wakabayashi, T. *J. Am. Chem. Soc.* **2000**, *122*, 1762−1775. Tobe, Y.; Nakanishi, H.; Sonoda, M.; Wakabayashi, T.; Achiba, Y. *Chem. Commun.* **1999**, 1625−1626. Tobe, Y.; Nakagawa, N.; Naemura, K.; Wakabayashi, T.; Shida, T.; Achiba, Y. *J. Am. Chem. Soc.* **1998**, *120*, 4544−4545.

(28) Bunz, U. H. F.; Roidl, G.; Altmann, M.; Enkelmann, V.; Shimizu, K. D. *J. Am. Chem. Soc.* **1999**, *121*, 10719−10726.

(29) Tykwinski, R. R.; Diederich, F.; Gramlich, F.; Seiler, P. *Helv. Chim. Acta* **1996**, *79*, 634−645.

(30) Fallis, A. G. *Can. J. Chem.* **1999**, *77*, 159−177.

(31) Goroff, N. S. *Acc. Chem. Res.* **1996**, *29*, 77−83.

(32) Meier, H. *Adv. Strain Org. Chem.* **1991**, *1*, 215−272.

(33) Misumi, S.; Kaneda, T. In *The Chemistry of the Carbon−Carbon Triple Bond Part 2*; Patai, S., Ed.; John Wiley & Sons: Chichester, 1978; pp 713−737.

(34) (a) Gleiter, R.; Merger, R.; Chavez, J.; Oeser, T.; Irngartinger, H.; Pritzkow, H.; Nuber, B. *Eur. J. Org. Chem.* **1999**, 2841−2843. (b) Haberhauer, G.; Gleiter, R.; Irngartinger, H.; Oeser, T.; Rominger, F. *J. Chem. Soc., Perkin Trans. 2* **1999**, 2093−2097. (c) Gleiter, R.; Haberhauer, G.; Irngartinger, H.; Oeser, T.; Rominger, F. *Organometallics* **1999**, *18*, 3615−3622. (d) Stahr, H.; Gleiter, R.; Haberhauer, G.; Irngartinger, H.; Oeser, A. *Chem. Ber.* **1997**, *130*, 1807−1811. (e) Gleiter, R.; Merger, R. In *Modern Acetylene Chemistry*; Stang, P. J., Diederich, F., Eds.; VCH: Weinheim, 1995; pp 285−319. (f) Gleiter, R.; Schäfer, W.; Flatow, A. *J. Org. Chem.* **1984**, *49*, 372−374.

(35) (a) Scott, L. T.; Cooney, M. J. In *Modern Acetylene Chemistry*; Stang, P. J., Diederich, F., Eds.; VCH: Weinheim, 1995; pp 321−351. (b) Scott, L. T.; Cooney, M. J.; Otte, C.; Puls, C.; Haumann, T.; Boese, R.; Carroll, R. J.; Smith, A. B., III; de Meijere, A. *J. Am. Chem. Soc.* **1994**, *116*, 10275−10283.

(36) Matsuoka, T.; Negi, T.; Otsubo, T.; Sakata, Y.; Misumi, S. *Bull. Chem. Soc. Jpn.* **1972**, *45*, 1825−1833.

(37) (a) Toda, F.; Ando, T.; Kataoka, M.; Nakagawa, M. *Bull. Chem. Soc. Jpn.* **1971**, *44*, 1914−1916. (b) Kataoka, M.; Ando, T.; Nakagawa, M. *Bull. Chem. Soc. Jpn.* **1971**, *44*, 1909−1914. (c) Kataoka, M.; Ando, T.; Nakagawa, M. *Bull. Chem. Soc. Jpn.* **1971**, *44*, 177−184. (d) Ando, T.; Nakagawa, M. *Bull. Chem. Soc. Jpn.* **1971**, *44*, 172−177. (e) Toda, F.; Nakagawa, M. *Bull. Chem. Soc. Jpn.* **1961**, *34*, 874−786. (f) Toda, F.; Nakagawa, M. *Bull. Chem. Soc. Jpn.* **1961**, *34*, 862−874. (g) Toda, F.; Nakagawa, M. *Bull. Chem. Soc. Jpn.* **1960**, *33*, 223−230.

(38) Eisler, S.; Tykwinski, R. R. *Angew. Chem., Int. Ed.* **1999**, *38*, 1940−1943.

(39) Other examples of expanded radialenes: (a) Schreiber, M.; Tykwinski, R. R.; Diederich, F.; Spreiter, R.; Gubler, U.; Bosshard, C.; Poberaj, I.; Günter, P.; Boudon, C.; Gisselbrecht, J.-P.; Gross, M.; Jonas, U.; Ringsdorf, H. *Adv. Mater.* **1997**, *9*, 339−343. (b) Anthony, J.; Boldi, A. M.; Boudon, C.; Gisselbrecht, J.-P.; Gross, M.; Seiler, P.; Knobler, C. B.; Diederich, F. *Helv. Chim. Acta* **1995**, *78*, 797−817. (c) Boldi, A. M.; Diederich, F. *Angew. Chem., Int. Ed. Engl.* **1994**, *33*, 468−471.

(40) Baughman, R. H.; Yee, K. C. *J. Polym. Sci. Macromol. Rev.* **1978**, *13*, 219−239.

(41) *Polydiacetylenes*; Bloor, D., Chance, R. R., Eds.; Martinus Nijhoff: Dordrecht, 1985.

(42) Wegner, G. *Makromol. Chem., Suppl.* **1984**, *6*, 347−357. Wegner, G. *Makromol. Chem.* **1972**, *154*, 35−48.

(43) For a preliminary communication of **8c**−**e**, see: Tykwinski, R. R. *Chem. Commun.* **1999**, 905−906.

(44) Hopf, H. *Angew. Chem., Int. Ed. Engl.* **1984**, *23*, 948−960.

(45) Stang, P. J.; Fisk, T. E. *Synthesis* **1979**, 438−440.

Scheme 2. Attempted Synthesis of Macrocycle **9**

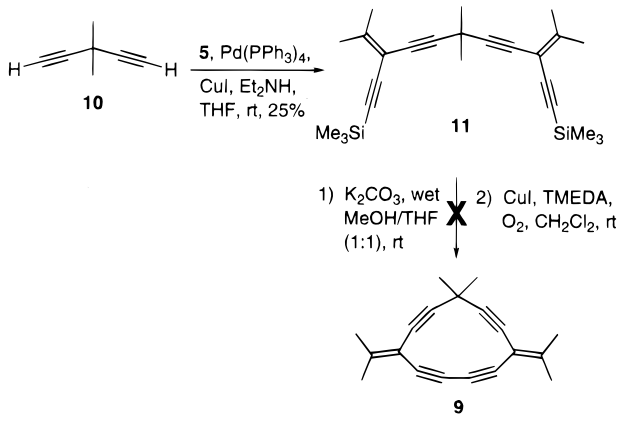

Scheme 3. Synthesis of Model Compound **12**

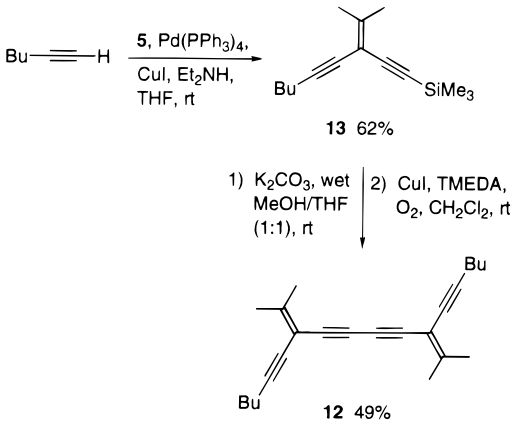

and $Pd(PPh_3)_4$.[46] The coupling process proceeds rapidly at room temperature and works equally well in either DMF or THF solvent. Overall yields of tethered enediynes **7a**−**e** were consistently modest with the mono-coupled product always isolated as the major byproduct.

Protodesilylation of **7a**−**e** with K_2CO_3 in MeOH/THF (1:1) for 2−3 h at room temperature affords the terminal alkynes. The desilylation proceeds in essentially quantitative yield with no evidence of byproduct formation. Following aqueous workup, these products were immediately carried on to the next step due to limited stability of desilylated product. Oxidative acetylenic coupling of the respective terminal alkynes of **7a**−**e** was accomplished in CH_2Cl_2 (ca. 0.001 M) with CuI and tetramethylethylenediamine (TMEDA).[47] Under these relatively dilute conditions, the cyclization reactions were generally complete in 2−5 h as monitored by TLC. Macrocycles **8a**−**e** were isolated as white solids in modest yields by column chromatography. Always apparent by TLC analysis were the acyclic oligomers that result from intermolecular oxidative coupling of the diyne precursors. Unfortunately, this intermolecular coupling reaction always competes effectively with intramolecular cyclization, regardless of the reaction concentration or conditions.

In an attempt to complete the series of strained cyclic dendralenes, the synthesis of highly strained **9** was also attempted (Scheme 2). In contrast to cycles **8a**−**e**, however, 3,3-dimethyl-1,4-pentadiyne (**10**)[35b] was used due to its ready availability and greater stability when compared to 1,4-pentadiyne. Coupling of **10** with vinyl triflate **5** gave tetrayne **11** as a white solid in acceptable yield of 25%. The trimethylsilyl groups of **11** were easily removed with K_2CO_3 to give the terminal diyne, which was then subjected to the oxidative cyclization conditions in CH_2Cl_2 (0.001 M) until TLC analysis no longer showed the presence of starting material. Clearly evident by TLC are numerous compounds of increasing polarity that likely correspond to linear oligomers formed from the oxidative coupling process. ^{1}H NMR and MS analysis of the resultant products, however, provided no evidence for the formation of the desired cycle **9**.

Synthesis of the acyclic model compound **12** (Scheme 3) began with the coupling of 1-hexyne to vinyl triflate **5**, affording enediyne **13** in good yield as a light yellow oil that slowly decomposes at room temperature when exposed to air. Protodesilylation of **13** (K_2CO_3 in MeOH/THF) gave the terminal acetylene that was directly subjected to oxidative coupling protocol to afford dimer **12** in 49% yield as a white solid.

Physical Characteristics and X-ray Crystal Structures. Acyclic tetrayne **12** has a sharp melting point at 71 °C and pure macrocycles **8a**−**e** are all thermally stable solids with melting or decomposition points above 100 °C. Cycles **8c** and **8e** show defined melting points of ca. 130 and 138 °C, respectively, whereas **8b** shows no melting point and decomposes at just under 110 °C. The most strained cycle, **8a**, shows darkening at 110 °C, finally blackening at 146 °C. Heating a single or microcrystalline sample of macrocycle **8d** to 135 °C gave an increasingly orange colored crystal that eventually melted reproducibly at 168 °C.[48]

The solid-state structures of the dendralenes **8a**−**e** and **12** were confirmed by X-ray crystallographic analysis. X-ray quality crystals were obtained by the diffusion of MeOH into $CHCl_3$ solutions (**8b**−**e** and **12**) or CH_2Cl_2 (**8a**) at 4 °C. ORTEP drawings of all structures are shown in Figure 1, whereas Tables 1−3 list crystallographic details and selected bond lengths and angles, respectively.[49]

Comparison of these six structures progressing from highly strained **8a** to relatively strain-free **8e** and acyclic **12** provides an understanding of the geometric changes as a result of the increasing ring strain. Empirically, macrocycles **8a**, **8d**, and **8e** are approximately symmetrical (C_2, C_s, and C_2, respectively), whereas the 13- and 14-carbon cycles **8b** and **8c** are distorted considerably from C_2 or C_s symmetry. This distortion in **8c** was initially thought to derive simply from crystal packing effects. Semiempirical structural analysis, however, provides a geometry for **8c** that is similar to the X-ray structure in which one "half" of the molecule is considerably more strained than the other.[50] This suggests the symmetry distortion in solid **8c** results from the inability of the four methylene linking groups to orient in a manner that equally disperses the ring strain, rather than from packing forces. The distortion of **8b** in the solid state is even

(46) Zhao, Y.; Tykwinski, R. R. *J. Am. Chem. Soc.* **1999**, *121*, 458−459.

(47) Hay, A. S. *J. Org. Chem.* **1962**, *27*, 3320−3321.

(48) Powder samples of **8d** show darkening at ca. 115 °C, and a reproducible melting point at ca. 155 °C. Continued heating gives rapid decomposition to a black solid at 165 °C. Differential scanning calorimetery of microcrystalline **8d** showed a distinct melting point at 160 °C, followed almost immediately by decomposition or polymerization. These observations suggested a topochemical reaction/polymerization involving the diacetylene moiety to a polydiacetylene (PDA) product. Analysis of the crystal packing of **8d**, however, shows the closest distance between atoms of the diacetylene groups to be greater than 7 Å, rendering PDA formation via a 1,4-addition pattern unlikely (see: Enkelmann, V. *Adv. Polym. Sci.* **1984**, *63*, 91−136). Analysis of the orange-colored material from the above experiments by ^{1}H NMR and MS shows predominantly the macrocycle **8d**. To date, the source of the discoloration remains unresolved, and investigations of the thermochemistry of **8d** are currently ongoing.

(49) The numbering scheme shown for structure **8c** in Figure 1 has been changed from that used in ref 43 to facilitate comparisons to the other structures.

(50) AM1 forcefield, MacSpartan Plus 1.1.9, Wavefunction, Inc., 1998.

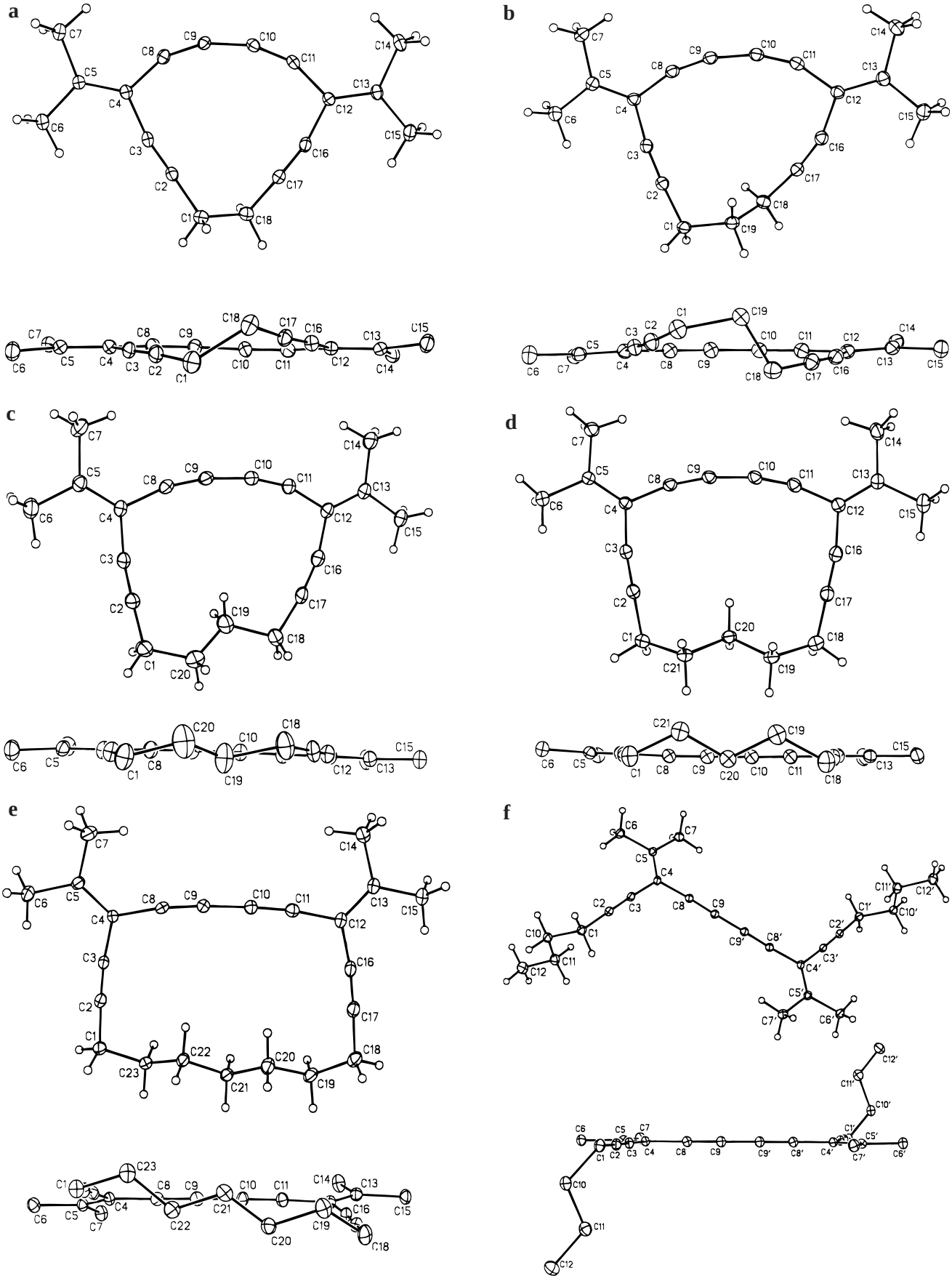

Figure 1. ORTEP drawings (20% probability level) of (a) **8a**, (b) **8b**, (c) **8c**, (d) **8d**, (e) **8e**, and (f) **12**.

more dramatic than that of **8c**. In the case of **8b**, calculations also predict a distortion from symmetry, albeit to a much smaller extent than observed experimentally in the crystal structure.[50] Raman spectroscopic analyses (vide infra) of both **8b** and **8c**

Table 1. Crystal, Intensity Collection, and Refinement Data for **8a**−**e** and **12**

	8a	**8b**	**8c**	**8d**	**8e**	**12**
lattice	monoclinic	triclinic	monoclinic	monoclinic	triclinic	triclinic
formula	$C_{18}H_{16}$	$C_{19}H_{18}$	$C_{20}H_{20}$	$C_{21}H_{22}$	$C_{23}H_{26}$	$C_{24}H_{30}$
formula wt	232.31	246.33	260.36	274.39	302.44	318.48
space group	$P2_1/n$[a]	$P\bar{1}$ (No. 2)	$P2_1/c$ (No. 14)	$P2_1/c$ (No. 14)	$P\bar{1}$ (No. 2)	$P\bar{1}$ (No. 2)
a/Å	6.5313(5)	8.3222(13)	9.2119(8)	8.4095(9)	12.2451(13)	7.2155(11)
b/Å	26.949(2)	8.3227(13)	12.5305(12)	8.3657(9)	12.6784(11)	7.6090(11)
c/Å	15.7798(14)	11.0132(17)	14.5747(10)	24.095(3)	13.5270(12)	10.0757(15)
α/°		97.810(3)			66.965(6)	106.604(3)
β/°	97.878(2)	96.413(3)	107.744(7)	92.601(2)	89.087(8)	103.335(3)
γ/°		91.112(3)			80.200(8)	100.228(3)
V/Å^3	2751.2(4)	750.5(2)	1602.3(2)	1693.4(3)	1901.4(3)	497.93(13)
Z	8	2	4	4	4	1
temp/K	193	193	213	193	193	193
radiation (λ, Å)	0.71073	0.71073	0.71073	0.71073	0.71073	0.71073
ρ(calcd)/g cm^{-3}	1.122	1.090	1.079	1.076	1.056	1.062
μ(Mo Kα)/mm^{-1}	0.063	0.061	0.061	0.060	0.059	0.059
2θ limit, deg	51.4	52.80	50	51.5	50	52.80
no. of data[b]	5217	3058	2814	3225	6334	2023
no. of obs data[c]	2076	2111	1399	1478	3139	1400
no. of parameters	333	176	185	194	423	111
R[d]	0.0526	0.0624	0.0762	0.0474	0.0672	0.0479
Rw[e]	0.1229	0.1760	0.1977	0.1106	0.1536	0.1325
GOF[f]	0.818	0.969	1.010	0.837	1.012	0.985

[a] A nonstandard setting of $P2_1/c$ (No. 14). [b] Unique data with $F_o^2 \geq -3\sigma(F_o^2)$. [c] $[F_o^2 \geq 2\sigma(F_o^2)]$. [d] $R = \sum||F_o| - |F_c||/\sum|F_o|$. [e] $Rw = \sum w(F_o^2 - F_c^2)^2/\sum w(F_o^4)^{1/2}$. [f] $[\sum w(F_o^2 - F_c^2)^2/(n-p)]^{1/2}$ (n = number of data; p = number of parameters varied; $w = [\sigma^2(F_o^2) + (a_oP)^2 + a_1P]^{-1}$, where $P = [\mathrm{Max}(F_o^2,0)^2 + 2F_c^2]/3$) and the coefficients a_o and a_1 are suggested by the least-squares program; **8a**, $a_o = 0.0388$, $a_1 = 0$; **8b**, $a_o = 0.1156$, $a_1 = 0$; **8c**, $a_o = 0.0764$, $a_1 = 0.5537$; **8d**, $a_o = 0.0374$, $a_1 = 0$; **8e**, $a_o = 0.0478$, $a_1 = 0.1698$; **12**, $a_o = 0.0726$, $a_1 = 0$.

Table 2. Selected Bond Lengths (Å) for **8a**−**e** and **12**

	8a[a]	**8a**[b]	**8b**	**8c**	**8d**	**8e**[a]	**8e**[b]	**12**
C(1)−C(2)	1.477(4)	1.458(4)	1.465(3)	1.461(5)	1.472(3)	1.472(5)	1.476(5)	1.468(2)
C(2)−C(3)	1.197(4)	1.185(3)	1.205(3)	1.180(5)	1.193(3)	1.193(4)	1.185(4)	1.195(2)
C(3)−C(4)	1.442(4)	1.454(4)	1.440(3)	1.455(5)	1.443(3)	1.444(5)	1.443(5)	1.444(2)
C(4)−C(5)	1.341(3)	1.345(3)	1.350(3)	1.336(4)	1.346(3)	1.348(4)	1.351(4)	1.357(2)
C(4)−C(8)	1.448(4)	1.442(4)	1.435(3)	1.439(5)	1.431(3)	1.441(4)	1.441(4)	1.4434(19)
C(8)−C(9)	1.195(4)	1.205(3)	1.208(3)	1.196(4)	1.198(3)	1.201(4)	1.200(4)	1.2038(18)
C(9)−C(10)	1.370(4)	1.381(4)	1.372(3)	1.378(5)	1.374(3)	1.382(5)	1.374(5)	1.377(3)[c]
C(10)−C(11)	1.209(3)	1.206(3)	1.209(3)	1.207(5)	1.202(3)	1.194(4)	1.198(4)	
C(11)−C(12)	1.442(4)	1.436(4)	1.438(3)	1.433(5)	1.436(3)	1.440(4)	1.439(5)	
C(12)−C(13)	1.339(3)	1.343(3)	1.347(3)	1.340(5)	1.342(3)	1.339(4)	1.350(4)	
C(12)−C(16)	1.446(4)	1.449(4)	1.454(3)	1.443(5)	1.441(3)	1.448(5)	1.446(5)	
C(16)−C(17)	1.198(4)	1.188(4)	1.192(3)	1.188(5)	1.197(3)	1.194(4)	1.188(5)	
C(17)−C(18)	1.467(4)	1.482(4)	1.463(3)	1.466(6)	1.469(3)	1.461(5)	1.465(5)	

[a] Data for molecule A of a crystallographically independent pair. [b] Data for molecule B of a crystallographically independent pair. [c] C(9)−C(9′).

Table 3. Selected Bond Angles (deg) for **8a**−**e** and **12**

	8a[a]	**8a**[b]	**8b**	**8c**	**8d**	**8e**[a]	**8e**[b]	**12**
C(1)−C(2)-C(3)	177.1(3)	175.4(3)	173.07(19)	176.6(4)	179.5(2)	174.2(4)	176.1(4)	179.19(15)
C(2)−C(3)-C(4)	167.9(3)	169.1(3)	170.66(19)	171.0(4)	170.5(2)	171.9(4)	173.0(4)	177.02(15)
C(3)−C(4)-C(5)	126.4(3)	125.8(3)	125.15(17)	125.2(3)	124.7(2)	124.2(3)	123.4(3)	123.34(13)
C(6)−C(5)-C(7)	116.6(2)	116.4(2)	116.65(17)	116.6(3)	116.77(18)	116.1(3)	116.7(3)	116.20(13)
C(3)−C(4)-C(8)	108.7(2)	108.5(2)	110.49(16)	110.9(3)	111.47(19)	112.4(3)	113.2(3)	114.77(12)
C(4)−C(8)-C(9)	157.1(3)	155.3(3)	163.7(2)	166.5(4)	168.0(2)	172.7(4)	172.2(4)	177.21(15)
C(8)−C(9)-C(10)	159.8(3)	159.5(3)	164.6(2)	169.0(4)	168.8(2)	177.3(4)	176.4(4)	179.1(2)[c]
C(9)−C(10)-C(11)	158.7(3)	160.1(3)	163.4(2)	168.2(4)	169.4(2)	176.6(4)	176.8(4)	
C(10)−C(11)-C(12)	156.7(3)	156.6(3)	156.88(19)	161.7(4)	166.4(2)	173.5(4)	172.5(4)	
C(11)−C(12)-C(13)	125.7(3)	126.0(3)	126.12(18)	125.4(4)	124.2(2)	123.0(3)	122.8(3)	
C(14)−C(13)-C(15)	116.6(2)	116.3(2)	117.19(17)	117.1(3)	115.7(2)	115.9(3)	115.9(3)	
C(11)−C(12)-C(16)	108.4(2)	108.9(2)	107.45(16)	108.4(3)	111.2(2)	112.7(3)	113.6(3)	
C(12)−C(16)-C(17)	168.5(3)	168.6(3)	161.6(2)	165.4(4)	170.4(2)	174.0(4)	173.0(4)	
C(16)−C(17)-C(18)	175.1(3)	174.0(4)	172.0(2)	170.5(4)	178.7(3)	173.7(4)	177.0(4)	

[a] Data for molecule A of a crystallographically independent pair. [b] Data for molecule B of a crystallographically independent pair. [c] C(8)−C(9)−C(9′).

display characteristics consistent with dissymmetric structures in solution. No evidence of symmetry distortion, however, was observed in solution on the time scale of ^{1}H or ^{13}C NMR analysis.

The relative planarity of each macrocycle in its preferred conformation is certain to influence its electronic behavior. The planarity of the conjugated portion of cycles **8a**−**e** and acyclic **12** in the solid state varies considerably and is not associated

Table 4. Selected ^{13}C NMR Shift Data (in ppm) for **8a**−**e** and **12**[a]

	C(2), C(17) $CH_2-\boldsymbol{C}\equiv C-$	C(3), C(16) $CH_2-C\equiv\boldsymbol{C}-$	C(4), C(12) $C\equiv C-\boldsymbol{C}(=C)-C\equiv C$	C(5), C(13) $C\equiv C-C(=\boldsymbol{C})-C\equiv C$	C(8), C(11) $-\boldsymbol{C}\equiv C-C\equiv C-$	C(9), C(10) $-C\equiv\boldsymbol{C}-C\equiv C-$
8a	90.3	81.2	103.5	145.0	105.1	86.5
8b	95.7	81.5	103.2	145.6	98.9	82.5
8c	94.6	80.7	102.8	146.9	90.4	80.0
8d	93.7	79.5	102.2	148.5	88.4	78.2
8e	93.8	79.1	101.8	151.3	81.7	75.9
12	93.1	76.4	100.9	156.0	79.5	75.4

[a] All spectra obtained in $CDCl_3$.

directly with decreasing ring size as might be expected. For each compound, the extent of twisting can be estimated by a dihedral angle between the two "arms" of the conjugated segment linked by the butadiyne moiety. Two planes, defined by C(3)−C(4)−C(5)−C(8) and C(11)−C(12)−C(13)−(16), respectively, provide this estimate of planarity. The conjugated portion of acyclic model compound **12** is completely planar, with a twist angle that is necessarily 180° based on solid state symmetry and the transoid orientation of the two alkylidene units about the butadiyne linker. For the most conformationally flexible macrocycle **8e**, with two crystallographically independent molecules A and B, the twist angle is greatest for molecule A at 22.2(2)° and somewhat smaller for molecule B at 12.7(3)°. The twist is approximately equal for **8c** and **8d** at 3.36(19)° and 2.82(13)°, respectively. The planarity of **8b** is quite distorted as a result of the dissymmetry of the molecule, with an angle of 8.22(16)°. Despite the considerably increased ring strain of **8a**, the twist angles at 7.0(2)° and 6.2(2)° for the two crystallographically independent molecules A and B, respectively, are greater than that of either **8c** or **8d**. Thus, increased twist and bond strain in the conjugated portion of **8a** is tolerated in order to accommodate the bond angles demanded by the two methylene groups.

Overall, the range of bond angles about the sp^3-hybridized carbons of the methylene groups of **8a**−**e** and **12** span a maximum of 119° to a minimum of 109° (both in **8c**). While the correlation between methylene bond angles and ring size is not linear, the general trend observed in these angles also relays the increased ring strain as evidenced by the mean values of for **8a**, **8b**, **8c**, **8d**, and **8e** of 115.9, 112.4, 115.0, 114.2, and 113.0°, respectively. By way of comparison, angles about the methylene carbons **12** are found, on average, to be 113.6°.

Structural analysis of the six molecules **8a**−**e** and **12** also shows that, in contrast to bond angles, the C−C, C=C, and C≡C bond lengths differ very little between the different structures. No discernible trends emerge that would correlate bond length to strain, and the bond lengths found in acyclic **12** are well within the same range as those of **8a**−**e**.

NMR Spectroscopic Properties. The ^1H and ^{13}C NMR spectra of macrocycles **8a**−**e** and acyclic **12** are completely consistent with their structures. None of the macrocycles **8a**−**e** shows any evidence of multiple conformers on the time scale of NMR measurements; the observed number of carbon resonances and line shapes clearly suggest the expected degeneracy for carbons related by C_2 or C_s symmetry. Unfortunately, however, the resonances for five of the six sp^2 and sp carbons fall within a similar range between 75 and 105 ppm. This fact made the empirical assignment of each resonance impossible.[51] Furthermore, due to the extensive multibond H−C coupling for these highly unsaturated molecules, shift assignments based on coupled, one-dimensional ^{13}C NMR techniques were also problematic as the values of ^3J, ^4J, and ^5J were similar in magnitude.[52]

The two-dimensional gradient heteronuclear multiple bond coherence (gHMBC) experiments for **8a**−**e** and **12**, however, were sufficient for assignment of all resonances for the conjugated carbon skeletons, as summarized in Table 4. In all cases, a similar strategy was used for interpretation of each gHMBC spectra. The alkylidene methyl protons of C(6)/C(15) and C(7)/C(14) for each molecule showed strong two- and three-bond ($^2J_{C-H}$ and $^3J_{C-H}$) correlations to the endo- and exocyclic alkylidene carbons C(4)/C(12) and C(5)/C(13), respectively (see X-ray structures in Figure 1 for numbering scheme). The exocyclic vinylidene carbons C(5)/C(13) are known to be significantly deshielded,[53] and thus C(4)/C(12) and C(5)/C(13) were assignable. Weaker four-bond correlations were observed between the alkylidene methyl protons and C(3)/C(16) and C(8)/C(11). In some cases, weak five-bond couplings to C(9)/C(10) and/or C(2)/C(17) were also observable. The $^2J_{C-H}$ and $^3J_{C-H}$ correlations between the propargylic methylene protons of C(1) and acetylenic carbons C(2) and C(3) identified these carbons. On the basis of the stronger ^4J coupling between C(3)/C(16) and the alkylidene methyl protons, C(2)/C(17) and C(3)/C(16) were thus assigned. The assignments of C(2)/C(17) and C(3)/C(16) were corroborated for **8b**, **8d**, and **12** by three-bond correlations between C(2) and the homopropargylic methylene protons of C(19) of **8b**, C(21) of **8d**, and C(10) of **12**. The $^5J_{C-H}$ coupling between the C(1) methylene protons and C(8) allowed the assignment of C(8)/C(11), leaving the assignment of C(9)/C(10) to the last ^{13}C NMR resonance.

The more shielded endocyclic alkylidene carbon C(4)/C(12) resonances are found over a rather narrow shift range between 100.9 and 103.5 ppm. For acyclic **12**, these carbons resonate at 100.9 ppm, and they are slightly deshielded to 101.8 ppm for the largest macrocycle **8e**. As the ring size is decreased from 17 to 12 upon moving from **8e** to **8a**, respectively, a deshielding is observed for these carbons to give values of 102.2 (**8d**), 102.8 (**8c**), 103.2 (**8b**), and 103.5 (**8a**). These shifts are consistent with the expected rehybridization at C(4)/C(12), as bond angle contraction for C(3)−C(4)−C(8) and C(11)−C(12)−C(16) imparts greater p-character to the σ-bonds of the ring and, consequently, more s-character to the olefin.[33,39b,54] Conversely, the chemical shifts of the exocyclic vinylidene C(5)/C(13) carbons are shifted significantly upfield as a function of strain, from the value observed for acyclic **12** at δ 156.0 to 151.3 (**8e**), 148.5 (**8d**), 146.9 (**8c**), 145.6 (**8b**), and 145.0 (**8a**).

A strong correlation is found between the crystallographic-determined bond angles and ^{13}C NMR shifts of the sp and sp^2 carbons. The angles α were calculated as an average of the X-ray angles at ^{13}C NMR degenerate carbons (Table 5). As shown in

(51) Using an empirical analysis, the ^{13}C NMR shifts of C(4)/C(12) for **8c**−**e** were incorrectly reported in ref 43.

(52) Kalinowski, H. O.; Berger, S.; Braun, S. *Carbon-13 NMR Spectroscopy*; John Wiley & Sons: Chichester, 1988.
(53) Neidlein, R.; Winter, M. *Synthesis* **1998**, 1362−1366.
(54) Wong, H. N. C.; Sondheimer, F. *Tetrahedron* **1981**, *37*, W99−W109.

Table 5. Averaged Angles α about sp- and sp²-Hybridized Carbon in **8a**−**e** and **12**

	α values (°)				
compd	C(2)/ C(17)	C(3)/ C(16)	C(4)/ C(12)[a]	C(8)/ C(11)	C(9)/ C(10)
8a[b]	175.4	168.5	108.6	156.4	159.5
8b	172.5	166.1	109.0	160.3	164
8c	173.6	168.2	109.7	164.1	168.7
8d	179.1	170.5	111.3	167.2	169.1
8e[b]	175.3	173.0	113.0	172.8	176.8
12	179.2	177.0	114.8	177.2	179.1

[a] C(3)−C(4)−C(8)/C(11)−C(12)−C(16). [b] Averaged over both crystallographically independent molecules A and B of the X-ray structure.

Figure 2, the relationship between the alkylidene bond angle α at C(3)−C(4)−C(8)/C(11)−C(12)−C(16) and the ^{13}C NMR resonances observed for *both* C(4)/C(12) and C(5)/C(13) is linear.

Changes in the relative bond order of the acetylenic moieties C(2)−C(3) and C(8)−C(9) (as well as C(10)−C(11) and C(16)−C(17), respectively) of **8a**−**e** and **12** are also easily monitored by their ^{13}C NMR resonances.[55] All acetylenic carbons experience consistent deshielding as ring strain is increased. A similar trend has been reported by Gleiter and co-workers for nonconjugated, cyclic diynes.[56] In particular, the carbons of the butadiyne carbons C(8)/C(11) and C(9)/C(10) experience significant deshielding as a result of increased ring strain. In the case of C(8)/C(11), the carbons are deshielded by 25 ppm upon going from acyclic **12** (79.5 ppm) to **8a** (105.1 ppm) as bond angles α are decreased from 177 to 156°, respectively. Concurrently, the C(9)/C(10) carbons are deshielded by 11 ppm, from δ 75.4 ppm in **12** to δ 86.5 ppm in **8a**, while the corresponding bond angles decrease from 179° in acyclic **12** to 159.6° in **8a**. The relationship between acetylenic bond angles and ^{13}C NMR shifts is nearly linear for all acetylenic carbons with the exception of C(2)/C(17).[55]

The only deviation from the above analysis is the anomalous ^{13}C NMR chemical shift observed for acetylenic carbons C(2)/C(17) of the most strained cycle **8a** (Table 4). This carbon resonance for **8a** is shielded by 5.4 ppm relative to **8b**, and by 3.5 ppm vs **8e**, which has the most similar bond angle with α = 175.3°. The origin of this shielding remains unclear. Based on the work of Gleiter and co-workers,[56,57] however, two possible influences emerge. The transannular distance between C(2) and C(17) is 3.08 Å for **8a**. This distance is at the limit of that required for through-space orbital overlap between these carbons and could potentially alter the chemical shift. The transannular distance between C(2) and C(17) for all other cycles is too large for such interactions to occur (e.g., it is already 4.04 Å in **8b**). Alternatively, shielding of C(2)/C(17) acetylenic carbons might result from through-bond interactions between the ethano bridge and the in-plane π-system. Based on photoelectron spectroscopic experiments, similar $\sigma-\pi$ electronic interactions have been reported in cycles such as 1,5-cyclooctadiyne, although no concurrent change in ^{13}C NMR chemical shift was reported for this molecule.[56]

Electronic Absorption Characteristics. Two distinct π-electron systems must be considered in the electronic absorption analysis of cyclic dendralenes **8a**−**e** and acyclic **12**. One system is composed of the acetylenic π-orbitals directed, more or less, in the molecular plane of each macrocycle (Figure 3a). The in-plane system of the butadiyne group is indicative of this system, and its electronic absorption should be observable at approximately 260 nm. Contributions to the in-plane butadiyne π-electron system via homoconjugation with the "pendant" alkynes are possible if the alkylidene bond angles were sufficiently constricted. Conversely, the out-of-plane π-electron system includes the eight carbons of the linearly conjugated ene−yne−yne−ene segment (Figure 3b). Interactions via cross conjugation[46] from the two pendant acetylenic units could influence the electronic absorption(s) of this π-electron system, which are expected in the lower energy region of each electronic absorption spectrum.

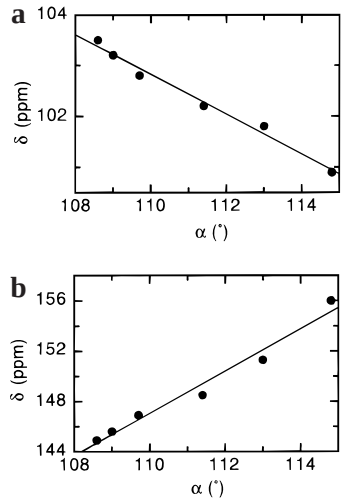

Figure 2. Plot of ^{13}C NMR chemical shift for (a) C(4)/C(12) and (b) C(5)/C(13) versus angle α C(3)−C(4)−C(8)/C(11)−C(12)−C(16).

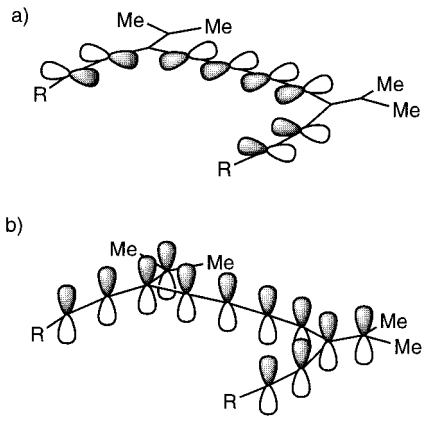

Figure 3. Schematic representation of the (a) in-plane and (b) out-of-plane p-orbital systems found in cyclic alkynes **8a**−**e** and acyclic **12**.

The UV absorption maxima of **8a**−**e** and acyclic analogue **12** are listed in Table 6, and the spectra for **8a**−**c** and **8c**−**e**, **12** are shown in Figure 4a and b, respectively. Empirically apparent are the similar energies of lower energy absorptions of **12** and those of macrocycles **8c**−**e** at ca. 290, 309, and 329 nm (Figure 4b), absorptions that arise from the out-of-plane π-electron system of each compound. The major difference in the spectrum of acyclic **12** versus cycles **8c**−**e** is the considerable broadening and lower ϵ-values of the low-energy absorptions for **12**. The latter is attributed to inhomogeneous broadening as a result of the rotational freedom of the alkylidene units about the butadiyne moiety of **12**. This gives both cisiod and transoid absorption

(55) See Supporting Information for correlations of ^{13}C NMR chemical shift data with bond angle α about acetylenic carbons C(2)/C(17), C(3)/C(16), C(8)/C(11), and C(9)/C(10).

(56) Gleiter, R.; Kratz, D.; Schäfer, W.; Schehlmann, V. *J. Am. Chem. Soc.* **1991**, *113*, 9258−9264.

(57) Gleiter, R.; Merger, R.; Irngartinger, H. *J. Am. Chem. Soc.* **1992**, *114*, 8927−8932.

Table 6. Selected UV Absorption Data (in nm) for **8a**−**e** and **12**[a]

	absorption maxima, λ_{max} (ϵ)				
8a	259 (30 000)	276 (21 100)	295 (13 900)	313 (29 900)	333 (26 000)
	262 (30 500)				
8b	260 (30 900)	275 (12 900)	292 (19 900)	311 (31 100)	331 (27 800)
8c	258 (25 000)	275 (10 700)	290 (18 600)	309 (31 500)	329 (29 500)
8d	259 (26 000)	275 (11 300)	291 (19 300)	309 (32 400)	329 (30 500)
8e	260 (29 000)	276 (8 400)	290 (15 700)	309 (26 500)	328 (24 500)
12	260 (21 700)	271 (19 100)	286 (13 900)	307 (15 800)	327 (12 500)

[a] All spectra obtained in $CHCl_3$. λ_{max} in nm and ϵ in L M^{-1} cm^{-1}.

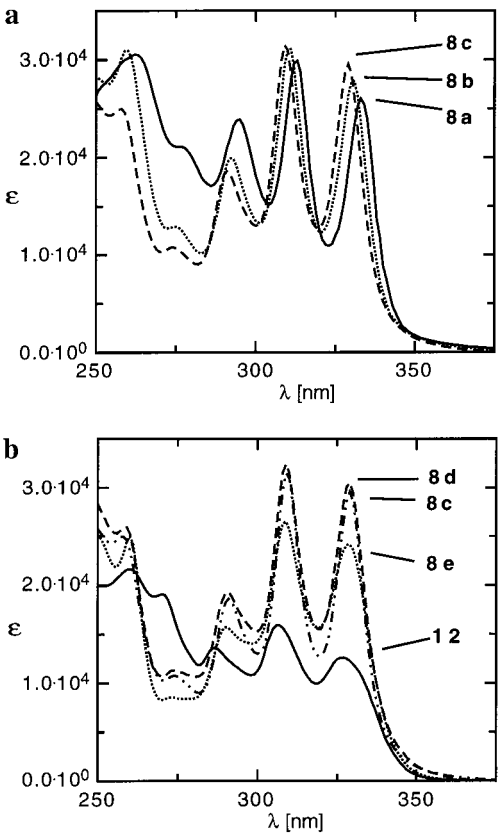

Figure 4. Electronic absorption spectra (ϵ [L M^{-1} cm^{-1}]) in $CHCl_3$ comparing (a) cyclic alkynes **8a**−**c** and (b) cyclic alkynes **8c**−**e** and acyclic **12**.

peaks in which the trans conformer absorbs at a slightly lower energy.[38] Peak broadening and lower ϵ-values are also observed for macrocycle **8e** relative to **8d** and **8c**. This is likely due to the more flexible 17-carbon cyclic framework of **8e**, which affords a lower overall molar absorptivity based on increased deviations from planarity allowed by the long $-(CH_2)_7-$ tether. Macrocycles **8d** and **8c** show the greatest ϵ-values, and this correlates well with the almost negligible twist angles (2.82(13)° and 3.36(19)°, respectively) observed in the solid state for the conjugated portions of these molecules. Molar absorptivitiy for the most strained systems **8b** and **8a** is diminished relative to **8c** as twisting increases to accommodate the shorter $-(CH_2)_3-$ and $-(CH_2)_2-$ tethers in these conformationally restricted macrocycles.

Whereas the lower energy electronic absorptions for **8c**−**e** show little variation in energies, further increasing ring strain on going from **8c** to **8b** to **8a** results in a consistent bathochromic shift for all three low-energy absorptions. For example, λ_{max} of **8c** at 329 nm shifts to 331 nm in **8b** and to 333 nm in **8a** (Figure 4a). As it is the overlap of the eight conjugated out-of-plane carbon sp and sp^2 π-orbitals of the ene−yne−yne−ene segment that yields these absorption bands, this bathochromic shift evidently derives from increased ring strain rather than homoconjugation (vide infra), which would arise from the in-plane π-system. It is not unreasonable to expect that the significant distortion from linearity in **8a** and **8b** slightly diminishes the overlap of the out-of-plane π-orbitals of these molecules. This has the effect of raising the energy of the HOMO to a slightly greater extent than that of the LUMO, resulting in a slightly lower energy transition.[11] The red-shifted λ_{max} observed for **8a** and **8b** contrasts results reported for *o,o′*-bridged polymethylene ether derivatives of diphenylacetylenes, **14**, the most structurally related system to be rigorously studied, to the best of our knowledge.[11,37a,e,f] In this case, a decrease in ring size for **14** from a planar, rigid structure ($n = 5$) to a strained, planar derivative ($n = 3$) afforded a hypsochromic shift of 12 nm in the lowest energy absorption. Modeling predicted that the p-orbitals contributing to conjugation, including the phenyl rings, are held parallel regardless of the magnitude of strain; thus, the observed blue shift was attributed entirely to ring strain.[37a,f] Conversely, ring contraction in the *p,p′*-bridged system **15** gave a bathochromic shift in λ_{max} from 342.5 nm in the strain-free, planar structure ($n = 18$) to 345.5 nm in a highly strained and nonplanar structure ($n = 13$).[37a,b] In contrast to cycles **14**, however, the conjugated p-orbitals in cycles **15** are no longer parallel as the two benzene groups deviate from coplanarity in more strained derivatives. It was suggested that this nonparallel alignment was responsible for the red shift in λ_{max} for the more strained derivatives of **15**. It is thus clear that the electronic characteristics in cross-conjugated systems cannot be effectively predicted on the basis of established studies of linearly conjugated systems.

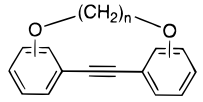

14 *o,o′*-, n = 3-6
15 *p,p′*-, n = 13-18

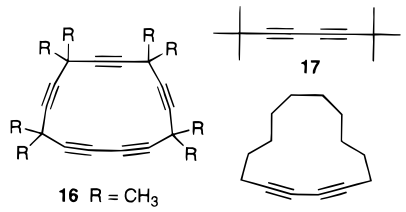

16 R = CH_3

17

18

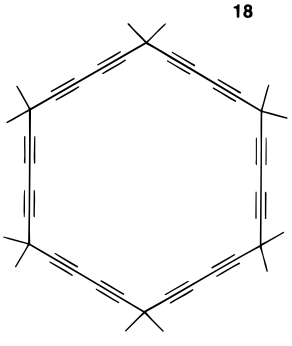

19

It has been shown for a series of [6]-, [4]-, and [3]radialenes that increased rigidity and enforced planarity as a function of ring contraction gives a decreasing absorption energy in a trend similar to that observed for **8a**−**e**,[58] although the overall

(58) Hopf, H.; Maas, G. *Angew. Chem., Int. Ed. Engl.* **1992**, *31*, 931−954.

conjugation length is lower in the radialenes than in **8a**−**e**. Slight changes in the electronic absorption spectra as a function of ring size have also been reported for expanded radialenes, which contain a similar ene−yne−yne−ene moiety as **8a**−**e**.[39b] The degree of strain, planarity, and steric interactions in these systems, however, is unknown and makes meaningful comparisons impossible.

The UV spectrum of the smallest dendralene **8a** shows evidence of homoconjugation, which affects the absorption of the in-plane butadiyne π-system at ca. 260 nm.[35b,59] Specifically, cycles **8b**−**e** and acyclic **12** all display this high-energy absorbance at 258−260 nm with increased broadening as the ring size is contracted. The spectrum of the highly strained cycle **8a** shows a substantially broadened peak at 263 nm, in addition to the shoulder absorption at 259 nm. This bathochromic shift in **8a** relative to **8b**−**e** and **12** is most reasonably ascribed to a through-space interaction of the in-plane π-orbital system of **8a** as a result of significantly deceased alkylidene bond angles. These results mirror those found previously for cycle **16**.[35b] As a result of homoconjugation, strained cycle **16** (λ_{max} = 266 nm) shows bathochromic shifts of 11 nm versus acyclic **17** (λ_{max} = 255 nm) and 10 nm versus the cyclic diyne **18** (λ_{max} = 256 nm). Also supporting the premise of homoconjugation in **16** is the 7 nm bathochromic shift of λ_{max} for **16** versus unstrained percycline **19** (λ_{max} = 259 nm). The interior bond angles of the saturated carbons of **16** at 103.8° are only 5° smaller than the alkylidene angles of **8a** at 108.6°.[35b]

Raman Spectroscopic Properties. Raman and resonance Raman characterization of electronic structures have been reported for cycloalkynes.[1,18] None of these studies, however, has addressed the electronic structure of macrocyclic molecules with extended or cross conjugation. Either or both of these attributes should afford significantly different electronic structures relative to less functionalized and linearly conjugated examples. In previous investigations, correlations have been observed between lower vibrational frequencies and smaller C−C≡C bond angles, and these observations were attributed to rehybridization of the central carbon atom from sp toward sp^2. The rehybridization results in a lower force constant of the C≡C stretch and altered coupling between the C≡C and C−C stretches as the C−C≡C bond angle varies. These observations are variations of Badger's rule,[60,61] which empirically relates diatomic stretching frequencies to the electronic nature of the bond. These preceding results all suggest that Raman spectroscopy should be a useful probe of electronic structure in our novel cross-conjugated enyne macrocycles.

Raman spectra of cross-conjugated enynes **8a**−**e** and **12** are shown for the 900−1700 cm^{-1} region in Figure 5 and for the 1400−2300 cm^{-1} region in Figure 6. The 900−1700 cm^{-1} spectral region contains contributions from C−C and C═C stretches and C−H deformations, whereas the 2100−2300 cm^{-1} spectral region contains contributions only from C≡C stretches. The Raman spectra are of good quality, although the spectrum of **8b** exhibits a slightly lower signal-to-noise ratio than the other spectra due to fluorescence in this sample. This fluorescence, however, decayed after several minutes in the laser beam, indicating that it likely originates from the presence of a small amount of fluorescent impurity rather than from the dendralene.[62]

Examination of the spectra in Figures 5 and 6 reveals some important trends. The spectra all exhibit the greatest intensity

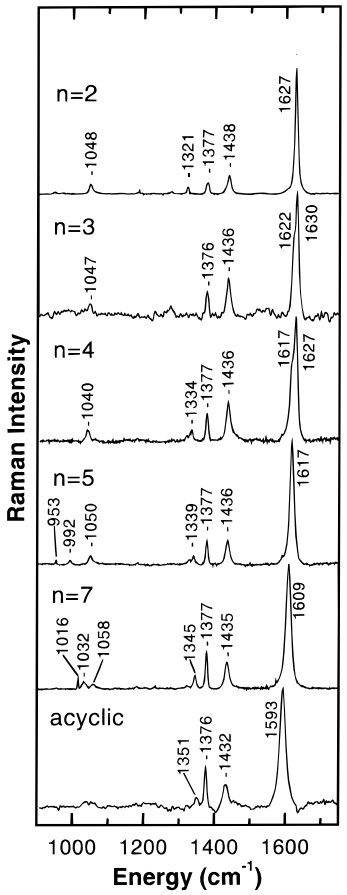

Figure 5. Raman spectra of cross-conjugated macrocycles **8a**−**e** and acyclic **12** in the 900−1700 cm^{-1} spectral region, displaced vertically for clarity. Typical accumulation times were 15 min; *n* is number of methylene groups.

in the C≡C stretch(es), followed closely by the C═C stretch(es); both the C−C stretches and C−H deformations, probably arising from the methylene groups, are much less intense. These intensities are to be expected, as the double and triple bonds are much more polarizable than the methylene groups.

Close inspection of the C═C and C≡C stretches reveals frequency shifts and mode splittings as a function of the increased ring strain upon moving from unstrained **12** to strained **8a**, consistent with the altered electronic structure exhibited in the crystal structure, and both ^{13}C NMR and electronic absorption spectra. In molecules **8b** and **8c**, with three and four methylene groups, respectively, the C═C and C≡C modes are significantly split, indicating either an inhomogeneity in the sample (e.g., different conformers) or nonequivalence in two or more similar bonds in the molecule. As the X-ray structures of **8b** and **8c** clearly show nonsymmetrical geometry in the solid state for both molecules, it is apparent that in solution there are indeed two nonequivalent sets of sp and sp^2 bonds. As discussed above, this premise has been supported by a semiempirical analysis that also predict nonsymmetrical geometries for **8b** and **8c**.

For the C═C stretching frequencies (Figure 5), a clear shift to lower frequency is observed, indicating a lower bond order for the alkylidene group as ring strain is decreased. The shift in olefinic stretching frequencies nicely complements the trend observed in the ^{13}C NMR shift data, relating the double bond order as a function of ring strain. Indeed, a plot (not shown) of the C═C stretching frequencies for **8a**−**e** (frequencies averaged for **8b** and **8c**) versus the ^{13}C NMR shifts of C(4)/C(12) and C(5)/C(13) affords a linear relationship in both cases, with

(59) Armitage, J. B.; Whiting, M. C. *J. Chem. Soc.* **1952**, 2005−2010.
(60) Badger, R. M. *J. Chem. Phys.* **1934**, *2*, 128−131.
(61) Gordy, W. *J. Chem. Phys.* **1946**, *14*, 305−320.
(62) No impurity could be detected by TLC or ^1H NMR analysis.

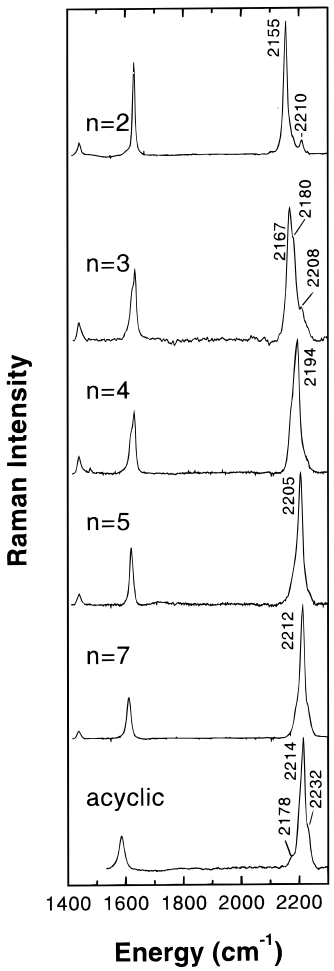

Figure 6. Same as Figure 5, but in the 1400−2300 cm^{-1} spectral region.

correlation coefficients of 0.975 and 0.999, respectively.[63] Likewise, a plot (not shown) of the alkylidene bond angles α for C(3)−C(4)−C(8)/C(11)−C(12)−C(16) versus olefinic stretching frequency is also linear, with a correlation coefficient of 0.995.[64] Analogous trends in bond order as a function of ring strain have been reported in radialenes[58] and have been well studied for alicyclic ketones and alkylidene cycloalkanes.[65] In contrast, however, the current study extends the usefulness of Raman analysis for the study of macrocycles with increased conjugation and potential materials applications.

The C≡C stretching frequency (or frequencies) of the strained dendralenes monotonically increases upon going from the **8a** to acyclic **12**, indicating a greater bond order as ring strain is decreased. The trend observed for C≡C stretching frequency (or frequencies) mirrors those observed for ^{13}C NMR shifts of the acetylenic carbons and averaged bond angles α, although with more substantial deviations from linearity than described above in the analysis of C═C data.[1,18,66] Smaller deviations have been observed in cycloalkynes[1] and are attributed in the present case to altered vibrational mixing, which will change not only the force constant, but also the vibrational character of the normal mode.

Conclusions

We have presented the synthesis and comprehensive analyses for a series of cyclic dendralenes that relate structural and spectroscopic attributes as a function of ring strain. The degree of bond angle deformation that is clearly depicted in the respective X-ray structures for each molecule can be directly correlated to trends in Raman and ^{13}C NMR spectroscopic data and directly reflect the varying electronic structure. Despite significant deviations from optimal bond angles for cycles **8a** and **8b**, ring strain exerts only a small influence on the electronic absorption spectra of these compounds, giving a slight bathochromic shift in λ_{max} values. In the most strained cycle **8a**, dramatic angle contraction affords changes in the higher energy region of the UV spectrum that can be attributed to the through-space π-orbital interactions of homoconjugation. A number of the correlations between strain and spectroscopic properties described herein show empirical trends similar to those reported for other less conjugated or nonconjugated systems. Other strain-based correlations for **8a**−**e**, such as the bathochromic shift in electronic absorptions of strained dendralenes **8a**,**b**, however, run contrary to previously reported studies and demonstrate the need for thorough analysis of new and structurally unprecedented systems. The structural relationships between these six homologous molecules **8a**−**e** and **12** provide a solid basis for a better understanding of the fundamental properties of these and future cross-conjugated macrocycles.

Experimental Section

General. Reagents were purchased reagent grade from commercial suppliers and used without further purification. THF was distilled from sodium/benzophenone ketyl. 1-Hexyne and **6b**−**d** were purchased from Aldrich and **6a** from GFS chemicals. Compounds **5**,[45] **10**,[35b] and **6e**[67] were prepared as described. Anhydrous $MgSO_4$ was used as the drying agent after aqueous workup. Evaporation and concentration in vacuo was done at H_2O-aspirator pressure. All reactions were performed in standard, dry glassware under an inert atmosphere of N_2. A positive pressure of N_2 was essential to the success of all Pd-catalyzed reactions. Degassing of solvents was accomplished by vigorously bubbling N_2 through the solution for at least 45 min. Column chromatography employed silica gel-60 (230−400 mesh) from General Intermediates of Canada. Thin-layer chromatography (TLC) used aluminum sheets covered with silica gel-60 F_{254} from Macherey-Nagel; visualization was done by UV light or $KMnO_4$ stain. Melting points were determined with a Gallenkamp apparatus and are uncorrected. UV/vis spectra were recorded using a Pharmacia Biotech Ultrospec 3000 at room temperature; λ_{max} is reported in nm (ϵ in L M^{-1} cm^{-1}). IR spectra (cm^{-1}) were obtained on a Nicolet Magna-IR 750 (neat) or Nic-Plan IR Microscope (solids). ^1H and ^{13}C NMR studies were done with Varian Gemini-300 or -500 and Bruker AM-300 instruments, at room temperature in $CDCl_3$; solvent peaks (7.24 ppm for ^1H and 77.0 ppm for ^{13}C) are used as reference. gHMBC spectra were recorded using a Varian Gemini-500 instrument at room temperature in $CDCl_3$. EI MS (*m*/*z*) were obtained with a Kratos MS50 instrument. Pro Fit Version 5.1.2 from QuantumSoft (Zürich, Switzerland) was used for all data analyses.

Raman. Room-temperature Raman spectra of the cross-conjugated enynes **8a**−**e** and **12** were obtained with 1-mL solutions of the sample in CCl_4. Raman scattering was excited by spherically focusing the 514.5-nm laser line from an Ar ion laser (Coherent, Santa Clara, CA) onto a spinning 5-mm NMR tube containing the sample solution in a 135° backscattering geometry. The laser power was typically 200 mW. Multichannel detection of the resonance Raman scattering was ac-

(63) See Supporting Information for correlations of (a) olefinic Raman frequencies with ^{13}C NMR chemical shift data for carbons C(4)/C(12) and C(5)/C(13), and b) olefinic Raman frequencies with bond angle α C(3)−C(4)−C(8)/C(11)−C(12)−C(16).

(64) See Supporting Information for correlations of acetylenic Raman frequencies with bond angle α about carbons C(8)/C(11) and C(9)/C(10).

(65) Bellamy, L. J. *Advances in Infrared Group Frequencies*; Methuen: London, 1968.

(66) Detert, H.; Meier, H. *Liebigs Ann./Recl.* **1997**, 1565−1570.

(67) Brandsma, L. *Preparative Acetylenic Chemistry*, 2nd ed.; Elsevier: Amsterdam, 1988.

complished with a liquid nitrogen-cooled CCD detector (Princeton Instruments, Trenton, NJ) connected to the first half of a double monochromator (Spex Industries, Metuchen, NJ). Rejection of the Rayleigh line was accomplished by a holographic filter (Kaiser Optical Systems, Ann Arbor, MI). Spectral slit widths were 5−7 cm^{-1}. Frequency calibration was performed by measuring Raman scattering of solvents of known frequencies (acetone, acetonitrile, and ethanol) and by measuring atomic emission lines from Kr and Ne lamps. Reported frequencies are accurate to ±2 cm^{-1}. The resonance Raman spectra were analyzed by using a 486DX2-66V computer (Gateway Computers, North Sioux City, SD). A CCl_4 solvent spectrum was subtracted from all solution spectra. The baselines were leveled by subtracting multiple joined line segments from the spectrum.

General Procedure for the formation of Tethered Enediynes. The appropriate diyne **6a**−**e** was added to a degassed solution of vinyl triflate **5** (2−2.1 equiv) in THF (20 mL). $Pd(PPh_3)_4$ (ca. 0.05 equiv) and Et_2NH (0.5−2 mL) were sequentially added, the solution was stirred for 5 min, CuI (ca. 0.15 equiv.) was added, and the solution was stirred until TLC analysis no longer showed progression toward the product (1−3 h.). In a number of cases, reaction progress ceased with a mixture of monocoupled product, product, and triflate all present in TLC analysis. Additional palladium catalyst or extended reaction times never effected additional product formation. Following completion of the reaction, ether and H_2O were added, the organic phase was separated, washed with saturated aqueous NH_4Cl (2 × 50 mL), and dried, and the solvent was removed in vacuo. Flash column chromatography gave the desired products.

3,10-Bis(trimethylsilylethynyl)-2,11-dimethyldodeca-2,10-diene-4,8-diyne (7a). Compound **7a** (0.034 g, 45%) was obtained as a white solid according to the general procedure from the reaction of 1,5-hexadiyne (0.050 mL of 4 M solution in pentane, 0.20 mmol), vinyl triflate **5** (0.13 g, 0.43 mmol), $Pd(PPh_3)_4$ (12 mg, 0.010 mmol), Et_2NH (1 mL), and CuI (4 mg, 0.02 mmol) in THF (5 mL). R_f = 0.45 (5:1 hexanes/CH_2Cl_2). Mp = 80−82 °C. IR (solid): 2956, 2149, 1601, 1438 cm^{-1}. ^1H NMR ($CDCl_3$, 300 MHz): δ 2.64 (s, 4H), 2.03 (s, 6H), 2.02 (s, 6H), 0.23 (s, 18H). ^{13}C NMR ($CDCl_3$, 75.5 MHz): δ 154.7, 102.2, 101.4, 95.6, 90.5, 78.1, 22.6 (2×), 20.0, 0.1. EI HRMS: calcd for $C_{24}H_{34}Si_2$ 378.2199, found 378.2205.

3,11-Bis(trimethylsilylethynyl)-2,12-dimethyltrideca-2,11-diene-4,9-diyne (7b). Compound **7b** (0.059 g, 61%) was obtained as a white solid according to the general procedure from the reaction of 1,6-heptadiyne (0.024 g, 0.246 mmol), vinyl triflate **5** (0.147 g, 0.488 mmol), $Pd(PPh_3)_4$ (17 mg, 0.015 mmol), Et_2NH (0.5 mL), and CuI (7 mg, 0.04 mmol) in THF (6 mL). R_f = 0.15 (20:1 hexanes/CH_2Cl_2). Mp = 67−69 °C. IR ($CHCl_3$ cast): 2935, 2145, 1595, 1428 cm^{-1}. ^1H NMR ($CDCl_3$, 300 MHz): δ 2.53 (t, J = 7.1 Hz, 4H), 2.03 (s, 6H), 2.01 (s, 6H), 1.83 (p, J = 7.1 Hz, 2H), 0.23 (s, 18H). ^{13}C NMR ($CDCl_3$, 75.5 MHz): δ 154.1, 102.4, 101.5, 95.5, 91.3, 77.8, 28.0, 22.6 (2×), 18.8, 0.1. EI HRMS: calcd for $C_{25}H_{36}Si_2$ 392.2356, found 392.2357.

3,12-Bis(trimethylsilylethynyl)-2,13-dimethyltetradeca-2,12-diene-4,10-diyne (7c). Compound **7c** (0.135 g, 39%) was obtained as a white solid according to the general procedure from the reaction of 1,7-octadiyne (0.090 g, 0.85 mmol), vinyl triflate **5** (0.600 g, 2.00 mmol), $Pd(PPh_3)_4$ (49 mg, 0.042 mmol), Et_2NH (2 mL), and CuI (25 mg, 0.13 mmol) in DMF (25 mL). R_f = 0.45 (4:1 hexanes/CH_2Cl_2). Mp = 78−79 °C. IR (solid): 2958, 2229, 2150, 1459 cm^{-1}. ^1H NMR ($CDCl_3$, 300 MHz): δ 2.36 (t, J = 6.0 Hz, 4H), 1.97 (s, 6H), 1.95 (s, 6H), 1.66 (m, 4H), 0.17 (s, 18H). ^{13}C NMR ($CDCl_3$, 125 MHz): δ 153.9, 102.4, 101.6, 95.4, 91.9, 76.8, 27.9, 22.6 (2×), 19.1, 0.1. EI HRMS: calcd for $C_{26}H_{38}Si_2$ 406.2512, found 406.2505.

3,13-Bis(trimethylsilylethynyl)-2,14-dimethylpentadeca-2,13-diene-4,11-diyne (7d). Compound **7d** (0.137 g, 36%) was obtained as a light yellow oil according to the general procedure from the reaction of 1,8-nonadiyne (0.108 g, 0.900 mmol), vinyl triflate **5** (0.600 g, 2.00 mmol), $Pd(PPh_3)_4$ (150 mg, 0.130 mmol), Et_2NH (2 mL), and CuI (50 mg, 0.26 mmol) in DMF (30 mL). R_f = 0.2 (18:1 hexanes/CH_2Cl_2). IR ($CHCl_3$ cast): 2959, 2148, 1433 cm^{-1}. ^1H NMR ($CDCl_3$, 300 MHz): δ 2.34 (m, 4H), 1.97 (s, 6H), 1.95 (s, 6H), 1.55 (m, 6H), 0.17 (s, 18H). ^{13}C NMR ($CDCl_3$, 125 MHz): δ 153.9, 102.5, 101.6, 95.4, 92.2, 76.8, 28.3, 28.2, 22.6, 22.5, 19.5, 0.1. EI HRMS: calcd for $C_{27}H_{40}Si_2$ 420.2669, found 420.2668.

3,15-Bis(trimethylsilylethynyl)-2,16-dimethylheptadeca-2,15-diene-4,13-diyne (7e). Compound **7e** (0.158 g, 26%) was obtained as a light yellow oil according to the general procedure from the reaction of 1,10-undecadiyne (0.200 g, 1.35 mmol), vinyl triflate **5** (0.900 g, 3.00 mmol), $Pd(PPh_3)_4$ (50 mg, 0.043 mmol), Et_2NH (3 mL), and CuI (25 mg, 0.13 mmol) in DMF (30 mL). R_f = 0.45 (4:1 hexanes/CH_2Cl_2). IR ($CHCl_3$ cast): 2933, 2149, 1433 cm^{-1}. ^1H NMR ($CDCl_3$, 300 MHz): δ 2.32 (t, J = 6.9 Hz, 4H), 1.98 (s, 6H), 1.96 (s, 6H), 1.53 (m, 4H), 1.40 (m, 6H), 0.17 (s, 18H). ^{13}C NMR ($CDCl_3$, 75.5 MHz): δ 153.6, 102.5, 101.7, 93.5, 92.4, 76.6, 28.8, 28.7, 28.6, 22.5 (2×), 19.5, 0.1. EI HRMS: calcd for $C_{29}H_{44}Si_2$ 448.2982, found 448.2972.

3,9-Bis(trimethylsilylethynyl)-2,6,6,10-tetramethylundeca-2,9-diene-4,7-diyne (11). Compound **11** (0.090 g, 25%) was obtained as a white solid according to the general procedure from the reaction of dimethyl pentadiyne **10** (0.215 g, 0.907 mmol), vinyl triflate **5** (0.509 g, 1.69 mmol), $Pd(PPh_3)_4$ (52 mg, 0.045 mmol), Et_2NH (1.0 mL), and CuI (15 mg, 0.078 mmol) in THF (10 mL). R_f = 0.40 (5:1 hexanes/CH_2Cl_2). Mp = 104−106 °C. IR (CH_2Cl_2 cast): 2960, 2249, 2153, 1439 cm^{-1}. ^1H NMR ($CDCl_3$, 300 MHz): δ 1.98 (s, 6H), 1.96 (s, 6H), 1.56 (s, 6H), 0.18 (s, 18H). ^{13}C NMR ($CDCl_3$, 75.5 MHz): δ 155.1, 102.1, 101.3, 95.7, 95.4, 76.4, 31.3, 27.2, 22.7, 22.6, 0.1. EI HRMS: calcd for $C_{25}H_{36}$ Si_2 392.2356, found 392.2354.

3-Trimethylsilylethynyl-2-methylnon-2-en-4-yne (13). Compound **13** (0.103 g, 62%) was obtained as a light yellow oil according to the general procedure from the reaction of excess 1-hexyne (0.302 g, 3.67 mmol), vinyl triflate **5** (0.214 g, 0.714 mmol), $Pd(PPh_3)_4$ (24 mg, 0.021 mmol), Et_2NH (1.0 mL), and CuI (11 mg, 0.058 mmol) in THF (5.0 mL). R_f = 0.59 (5:1 hexanes/CH_2Cl_2). IR (CH_2Cl_2 cast): 2932, 2149, 1432 cm^{-1}. ^1H NMR ($CDCl_3$, 300 MHz): δ 2.32 (t, J = 6.9 Hz, 2H), 1.98 (s, 3H), 1.96 (s, 3H), 1.45 (m, 4H), 0.90 (t, J = 7.2 Hz, 3H), 0.17 (s, 9H). ^{13}C NMR (C_6D_6, 75.5 MHz): δ 152.6, 103.4, 102.8, 95.2, 92.6, 77.9, 30.8, 22.2, 22.1, 22.0, 19.2, 13.4, 0.1. EI HRMS: calcd for $C_{15}H_{24}Si$ 232.1647, found 232.1638.

General Procedure for Oxidative Coupling. A mixture of the appropriate enediyne **7a**−**e** or **13** and K_2CO_3 (ca. 10 mg) in wet THF/MeOH (1:1, 15−20 mL) was stirred at room temperature until TLC analysis showed complete conversion to the desilylated derivative (0.5−2 h). Ether and saturated aqueous NH_4Cl were added, and the organic phase separated, washed with saturated aqueous NH_4Cl (2 × 50 mL), dried, reduced to ca. 1 mL, and added to CH_2Cl_2 to give a solution of 1−3 mM. Catalyst [CuI (50 mg, 0.26 mmol) and TMEDA (75 mg, 0.65 mmol) in CH_2Cl_2 (2 mL), stirred until homogeneous] was added and the mixture stirred at room temperature under air until TLC analysis no longer showed the starting material (ca. 1−5 h). The solution was concentrated in vacuo to ca. 5 mL, ether and H_2O were added, the organic phase was separated, washed with saturated aqueous NH_4Cl (2 × 50 mL), and dried, and the solvent was removed in vacuo. Flash column chromatography and/or precipitation from MeOH gave the desired product.

5,12-Diisopropylidenecyclododeca-1,3,6,10-tetrayne (8a). Compound **8a** (0.0122 g, 32%) was obtained as a white solid according to the general oxidative coupling procedure using **7a** (0.0622 g, 0.164 mmol), CuI (60 mg, 0.32 mmol), and TMEDA (0.1 mL) in CH_2Cl_2 (60 mL). R_f = 0.55 (2:1 hexanes/CH_2Cl_2). Sample discolors at 110 °C, decomposes at 146 °C. IR (CH_2Cl_2 cast): 2907, 2149, 1622, 1340 cm^{-1}. ^1H NMR ($CDCl_3$, 300 MHz): δ 2.65 (s, 4H), 1.98 (s, 6H), 1.90 (s, 6H). ^{13}C NMR ($CDCl_3$, 125 MHz): δ 145.0, 105.1, 103.5, 90.3, 86.5, 81.2, 23.4, 22.1, 19.8. UV/vis ($CHCl_3$): λ (ϵ) 333 (26 000), 313 (29 900), 295 (13 900), 276 (21 100), 263 (30 500), 259 (30 000) nm. EI HRMS: calcd for $C_{18}H_{16}$ 232.1252, found 232.1253.

5,13-Diisopropylidenecyclotrideca-1,3,6,11-tetrayne (8b). Compound **8b** (0.0074 g, 20%) was obtained as a white solid according to the general oxidative coupling procedure using **7b** (0.0593 g 0.151 mmol), CuI (62 mg, 0.32 mmol), and TMEDA (0.1 mL) in CH_2Cl_2 (60 mL). R_f = 0.34 (5:1 hexanes/CH_2Cl_2). Sample discolors at 100 °C, decomposes at 109−111 °C. IR ($CHCl_3$ cast): 2904, 2145, 1617, 1346 cm^{-1}. ^1H NMR ($CDCl_3$, 300 MHz): δ 2.45 (t, J = 6.2 Hz, 4H), 2.00 (p, J = 6.2 Hz, 2H), 1.90 (s, 6H), 1.85 (s, 6H). ^{13}C NMR ($CDCl_3$, 125 MHz): δ 145.6, 103.2, 98.9, 95.7, 82.5, 81.5, 28.0, 23.1, 22.2, 19.8. UV/vis ($CHCl_3$): λ (ϵ) 331 (27 800), 311 (31 100), 292 (19 900), 275

(12 900), 259 (30 900) nm. EI HRMS: calcd for $C_{19}H_{18}$ 246.1409, found 246.1408.

5,14-Diisopropylidenecyclotetradeca-1,3,6,12-tetrayne (8c). Compound **8c** (0.0062 g, 34%) was obtained as a white solid according to the general oxidative coupling procedure using **7c** (0.0285 g, 0.0701 mmol), CuI (28 mg, 0.15 mmol), and TMEDA (0.5 mL) in CH_2Cl_2 (30 mL). R_f = 0.34 (5:1 hexanes/CH_2Cl_2). Mp = 129−130 °C. IR (solid): 2905, 2214, 2192, 2118, 1618, 1334 cm^{-1}. ^1H NMR ($CDCl_3$, 300 MHz): δ 2.35 (m, 4H), 1.91 (s, 6H), 1.89 (s, 6H), 1.74 (AA′BB′, 4H). ^{13}C NMR ($CDCl_3$, 125 MHz): δ 146.9, 102.8, 94.6, 90.4, 80.7, 80.0, 29.2, 22.9, 22.2, 19.9. UV/vis ($CHCl_3$): λ (ϵ) 329 (29 500), 309 (31 500), 290 (18 600), 275 (10 700), 258 (25 000) nm. EI HRMS: calcd for $C_{20}H_{20}$ 260.1565, found 260.1564.

5,15-Diisopropylidenecyclopentadeca-1,3,6,13-tetrayne (8d). Compound **8d** (0.024 g, 34%) was obtained as a white solid according to the general oxidative coupling procedure using **7d** (0.110 g, 0.260 mmol), CuI (90 mg, 0.47 mmol), and TMEDA (0.15 mL) in CH_2Cl_2 (60 mL). R_f = 0.25 (9:1 hexanes/CH_2Cl_2). Solid turns orange at 135 °C and then melts 168 °C. IR (solid): 2905, 2215, 2130, 1617, 1349 cm^{-1}. ^1H NMR ($CDCl_3$, 300 MHz) δ 2.42 (t, J = 5.6 Hz, 4H), 1.92 (s, 6H), 1.89 (s, 6H), 1.70 (m, 2H), 1.54 (m, 4H). ^{13}C NMR ($CDCl_3$, 125 MHz): δ 148.5, 102.2, 93.7, 88.4, 79.5, 78.2, 29.8, 28.9, 22.9, 22.2, 19.9. UV/vis ($CHCl_3$): λ (ϵ) 329 (30 500), 309 (32 400), 291 (19 300), 275 (11 300), 259 (26 000) nm. EI HRMS: calcd for $C_{21}H_{22}$ 274.1722, found 274.1726.

5,17-Diisopropylidenecycloheptadeca-1,3,6,15-tetrayne (8e). Compound **8e** (0.006 g, 22%) was obtained as a white solid according to the general oxidative coupling procedure using **7e** (0.040 g, 0.089 mmol), CuI (30 mg, 0.16 mmol), and TMEDA (0.1 mL) in CH_2Cl_2 (30 mL). R_f = 0.4 (4:1 hexanes/CH_2Cl_2). Mp: 136−138 °C. IR (solid): 2931, 2227, 2133, 1604 cm^{-1}. ^1H NMR ($CDCl_3$, 300 MHz): δ 2.35 (m, 4H), 1.96 (s, 6H), 1.95 (s, 6H), 1.55 (m, 8H), 1.29 (m, 2H). ^{13}C NMR ($CDCl_3$, 125 MHz): δ 151.3, 101.8, 93.8, 81.7, 79.1, 75.9, 30.3, 29.6, 28.9, 22.6, 22.5, 19.6. UV/vis ($CHCl_3$): λ (ϵ) 328 (24 500), 309 (26 500), 290 (15 700), 276 (8 400), 260 (29 000) nm. EI HRMS: calcd for $C_{23}H_{26}$ 302.2035, found 302.2035.

7,11-Diisopropylideneoctadeca-5,8,10,13-tetrayne (12). Compound **12** (0.0346 g, 49%) was obtained as a white solid according to the general oxidative coupling procedure using **13** (0.103 g, 0.444 mmol), CuI (42 mg, 0.22 mmol), and TMEDA (1 mL) in CH_2Cl_2 (30 mL). R_f = 0.32 (2:1 hexanes/CH_2Cl_2). Mp = 71−72 °C. IR (CH_2Cl_2 cast): 2932, 2221, 2136, 1590, 1361 cm^{-1}. ^1H NMR ($CDCl_3$, 300 MHz): δ 2.33 (t, J = 6.9 Hz, 4H), 2.01 (s, 6H), 1.99 (s, 6H), 1.47 (m, 8H), 0.90 (t, J = 7.2 Hz, 6H). ^{13}C NMR ($CDCl_3$, 125 MHz): δ 156.0, 100.9, 93.1, 79.5, 76.4, 75.4, 30.8, 22.7, 22.0, 21.1, 19.1, 13.6. UV/vis ($CHCl_3$): λ (ϵ) 327 (12 500), 307 (15 800), 286 (13 900), 271 (19 100), 260 (21 700) nm. EI HRMS: calcd for $C_{24}H_{30}$ 318.2347, found 318.2349.

Acknowledgment. This work was supported by a GenScience Endowment from the University of Alberta (to R.R.T.) and by NSERC of Canada (R.R.T. and G.R.L.). We thank Dr. Tom Nakashima for extensive help with the ^{13}C NMR studies, and Ms. Navjot Chahal for making a number of the starting materials.

Supporting Information Available: X-ray structural data, ^1H, ^{13}C, and gHMBC NMR spectra for **8a**−**e** and **12**, and correlations of ^{13}C NMR chemical shift data, bond angles α, and Raman frequencies (PDF). This material is available free of charge via the Internet at http://pubs.acs.org.

JA000617G